Journal of Engineering and Technology Research Vol.1 (5), pp. 081-090, August, 2009
Available online at http:// www.academicjournals.org/JETR

Full Length Research Paper

Study of the thermal and spectral sensitivities of organic-inorganic fabrication materials based arrayed waveguide grating for passive optical network applications

Abd El–Naser A. Mohammed, Ahmed Nabih Zaki Rashed* and Abd El–Fattah A. Saad

Electronics and Electrical Communication Engineering Department, Faculty of Electronic Engineering, Menouf 32951, Menoufia University, Egypt.

Accepted 6 July, 2009

In the present paper, the study of the spectral and thermal sensitivities of the inorganic materials such as (Silica-doped, Lithium Niobate) materials and organic materials such as (PMMA Polymer) based waveguides employed in arrayed waveguide grating (AWG) in Passive Optical Networks (PONs) against spectral wavelength and ambient temperature variations. Moreover, we have investigated the best performance characteristics of the proposed three different fabrication materials based AWG for optical network applications over wide range of the affecting parameters.

Key words: Passive optical networks, arrayed waveguide grating, spectral sensitivity, thermal sensitivity.

INTRODUCTION

Wavelength division multiplexing passive optical network (WDM-PON) is attractive for future broadband access networks because they are capable of handling the ever-increasing demands of data bandwidth, provide enhanced security (Frigo et al., 1998), and provide scalability to support several local subscribers (Maier and Reisslein, 2004). In addition, there is no need for time-multiplexing and ranging protocols in WDM-PONs. In the implementation of practical WDM-PON networks, the most critical issue is how to reduce the cost. Wavelength reuse or source-free optical network units (ONUs) is a good idea to reduce the cost of the whole network. A few novel schemes for source-free ONUs have been demonstrated (Smit and Van Dam, 1996). Using the sub carrier multiplexing (SCM) modulation technique to carry the downstream data by optical sub carriers and wavelength reuse has been proposed and experimentally demonstrated in (Uetsuka, 2004; Tsuda et al., 1999; Kohtoku et al., 2002). In this scheme, the unmodulated optical carrier, carrying no information, was delivered to the ONU. The utilization of this optical carrier, all-optical power will be effectively utilized and highly efficient operation can be realized. For future WDM-PON networks, broadcasting the video service or providing triple-play services (TPS) including data, video, and voice transmission will be needed. Ref. (Lee, 2003) experimentally demonstrated a WDM-PON, which can provide the TPS with 155-Mb/s video, 1-Gb/s downstream data, and 1-Gb/s upstream data. In their network, they need to use a new light-wave source for upstream signal modulation. Passive optical networks (PONs) are well suited for regions that are relatively small in geographic extent and number of users. The arrayed waveguide grating (AWG) has seen considerable development in the past few years, primarily in the development of devices for use as wavelength division-multiplexed (WDM) channel demultiplexers and routers. In contrast, AWG devices have seen only limited use in time-domain applications. For example, mode-locked pulse inputs have been spectrally sliced to yield pulses in the tens of picoseconds range at the repetition rate of the mode-locked source laser, and super continuum sources have been sliced to yield multiple optical wavelengths for high-speed systems studies (Tsuda et al., 1999). Modified AWG devices have also been used for Fourier transform optical pulse shaping (Kohtoku et al., 2002).

Here, present a completely new functionality, in which the AWG produces bursts of femto second pulses repeated

*Corresponding author. E-mail: ahmed_733@yahoo.com. Tel.: +2 048-3660617. Fax: +2 048-3660-617.

repeating at a terahertz rate, with the pulse repetition rate determined by the AWG design rather than the input pulse repetition rate. Each input pulse to the AWG produces a burst of very high-repetition-rate pulses. In principle, if a high-repetition-rate short pulse source is used as the input, continuous, or quasi-continuous trains of very high-repetition-rate short pulses may be generated as in a rate-multiplication scheme. Furthermore, identical femto second pulse bursts with slightly shifted center wavelength are obtained at different output channels of the AWG (Birks et al., 1997). The lack of active components in the network enables rapid deployment, operational simplicity, and reduced maintenance requirements. Wavelength division multiplexing (WDM) is currently deployed in high-capacity, long-haul fiber-optic transmission systems to support multiple high-speed channels. WDM takes advantage of the enormous bandwidth offered by optical fiber while allowing individual wavelength channels to be utilized at bit rates suited to low-cost electronic components. In addition to the large bandwidth, WDM all-optical networks provide high-speed data transmission without need for intermediate-node electrical converters and are transparent with respect to the data formats used. Implementing WDM functions in an all-optical layer network requires versatile (van Eijkelenborg et al., 2001), reliable and high performance optical devices, particularly wavelength selective switches such as optical cross connects (OXCs) and optical add–drop multiplexers (OADMs). Such devices comprise a small number of components, including the multiplexer /demultiplexer (MUX/DEMUX), various switches and other functional devices. The arrayed waveguide grating (AWG) has become increasingly important in these types of channel-selective routing devices for WDM signals. The AWG is an imaging device that disperses the image field of an input waveguide onto an array of output waveguides. The desired diffraction properties are obtained through linear variation in the length of the arrayed waveguides. Arrayed-waveguide gratings (AWGs) (also known as wavelength grating routers) are often used as the central routing device in such networks due to their excellent wavelength reuse properties. It is assumed that delivering power to the core of the network is not possible, any active components (Humbert et al., 2003), such as transmitters, receivers, and switches, can be supported only at the users at the periphery of the network (Kakarantzas et al., 2002). Arrayed waveguide grating (AWG) devices can be used in a large variety of applications. They can act as multiplexer/demultiplexers of wavelength-division multiplexing (WDM) systems and wavelength routers (MA et al., 2004).

In the present study, we have investigated and analyzed theoretically and parametrically spectral and thermal sensitivities of organic-inorganic materials based AWG to be used in wavelength division multiplexing (WDM) passive optical networks. Moreover, the investigation of the best performance characteristics of the proposed three different fabrication materials based AWG for photonic network applications has been modeled over wide range of the affecting parameters.

THEORETICAL MODEL AND EQUATIONS ANALYSIS

Silica-doped Material (SiO_2 (1-x)+GeO_2(x))

The set of parameters required to completely characterrize the wavelength dependence of the refractive-index (n) is given, where Sellmeier equation of the refractive-index is in form:

$$n^2 = 1 + \frac{B_1\lambda^2}{\lambda^2 - B_2^2} + \frac{B_3\lambda^2}{\lambda^2 - B_4^2} + \frac{B_5\lambda^2}{\lambda^2 - B_6^2} \quad (1)$$

Where λ is the optical wavelength (μm), where the Sellmeier equation coefficients are (Fleming, 1985):

B_1= 0.691663+0.1107001* x, B_2= $(0.0684043+0.000568306 * x)^2 * (T/T_0)^2$, B_3= 0.4079426+0.31021588 * x, B_4= $(0.1162414+0.03772465 * x)^2 * (T/T_0)^2$, B_5= 0.8974749-0.043311091 * x, B_6= $(9.896161+1.94577 * x)^2$. Where x is the of germania mole fraction, T is the temperature of the material, K, and T_0 is the reference temperature (300 K). The differentiation of Equation 1 w. r. t. wavelength (λ) gives:

$$\frac{\partial n}{\partial \lambda} = -(\lambda/n)\left[\frac{B_1B_2^2}{(\lambda^2 - B_2^2)^2} + \frac{B_3B_4^2}{(\lambda^2 - B_4^2)^2} + \frac{B_5B_6^2}{(\lambda^2 - B_6^2)^2}\right] \quad (2)$$

In fact, the Spectral Sensitivity is defined as the following:

$$S_\lambda^n = \frac{\lambda}{n}\left(\frac{\partial n}{\partial \lambda}\right) \quad (3)$$

By substituting from Equation (2) into Equation (3) which yields:

$$S_\lambda^n = -\left(\frac{\lambda^2}{n^2}\right)\left[\frac{B_1B_2^2}{(\lambda^2 - B_2^2)^2} + \frac{B_3B_4^2}{(\lambda^2 - B_4^2)^2} + \frac{B_5B_6^2}{(\lambda^2 - B_6^2)^2}\right] \quad (4)$$

Also, the differentiation of Equation (1) w. r. t. Temperature (T) which yields:

$$\frac{\partial n}{\partial T} = \left(-\lambda^2/n\right)\left[\frac{B_1B_2\frac{\partial B_2}{\partial T}}{(\lambda^2 - B_2^2)^2} + \frac{B_3B_4\frac{\partial B_4}{\partial T}}{(\lambda^2 - B_4^2)^2} + \frac{B_5B_6\frac{\partial B_6}{\partial T}}{(\lambda^2 - B_6^2)^2}\right] \quad (5)$$

In fact, the Thermal Sensitivity is defined as the following:

$$S_T^n = \frac{T}{n}\left(\frac{\partial n}{\partial T}\right) \quad (6)$$

By substituting from Equation (5) into Equation (6) which yields:

$$S_T^n = -\left(\frac{T\lambda^2}{n^2}\right)\left[\frac{B_1B_2\frac{\partial B_2}{\partial T}}{\left(\lambda^2-B_2^2\right)^2}+\frac{B_3B_4\frac{\partial B_4}{\partial T}}{\left(\lambda^2-B_4^2\right)^2}+\frac{B_5B_6\frac{\partial B_6}{\partial T}}{\left(\lambda^2-B_6^2\right)^2}\right] \quad (7)$$

Lithium niobate ($LiNbo_3$) material

The refractive-index (n) of the Sellmeier equation of the form:

$$n^2 = A_1 + A_2H + \frac{A_3+A_4H}{\lambda^2-\left(A_5+A_6H\right)^2}+\frac{A_7+A_8H}{\lambda^2-A_9^2}-A_{10}\lambda^2 \quad (8)$$

Where λ is in μm and $H = T^2 - T_0^2$. T is the temperature of the material, K, and T_0 is the reference temperature and is considered 300 K. The set of parameters is recast (Jundt, 1997). A_1 = 5.35583, A_2 = 4.629 x 10^{-7}, A_3 = 0.100473, A_4 = 3.862 x 10^{-8}, A_5 = 0.20692, A_6 = -0.89 x 10^{-8}, A_7 = 100, A_8 = 2.657 x 10^{-5}, A_9 = 11.34927, and A_{10} = 0.015334. Equation (8) can be simplified as the following:

$$n^2 = A_{12} + \frac{A_{34}}{\lambda^2-A_{56}^2}+\frac{A_{78}}{\lambda^2-A_9^2}-A_{10}\lambda^2 \quad (9)$$

Where: $A_{12}=A_1+A_2H$, $A_{34}=A_3+A_4H$, $A_{56}=A_5+A_6H$, $A_{78}=A_7+A_8H$

Then, the differentiation of Equation (9) w. r. t Wavelength (λ) gives:

$$\frac{\partial n}{\partial \lambda} = \left(\frac{-\lambda}{n}\right)\left[\frac{A_{34}}{\left(\lambda^2-A_{56}^2\right)^2}+\frac{A_{78}}{\left(\lambda^2-A_9^2\right)^2}+A_{10}\right] \quad (10)$$

In fact, the spectral sensitivity is defined as the following:

$$S_\lambda^n = \frac{\lambda}{n}\left(\frac{\partial n}{\partial \lambda}\right) \quad (11)$$

By substituting from Equation (10) into Equation (11) which yields:

$$S_\lambda^n = -\left(\frac{\lambda^2}{n^2}\right)\left[\frac{A_{34}}{\left(\lambda^2-A_{56}^2\right)^2}+\frac{A_{78}}{\left(\lambda^2-A_9^2\right)^2}+A_{10}\right] \quad (12)$$

Also, the differentiation of Equation (9) w. r. t. Temperature (T) gives:

$$\frac{\partial n}{\partial T} = \left(\frac{T}{n}\right)\left[A_2+\frac{\left(\lambda^2-A_{56}^2\right)A_4+2A_6A_{56}A_{34}}{\left(\lambda^2-A_{56}^2\right)^2}+\frac{A_8}{\left(\lambda^2-A_9^2\right)}\right] \quad (13)$$

In fact, the Thermal Sensitivity is defined as the following:

$$S_T^n = \frac{T}{n}\left(\frac{\partial n}{\partial T}\right) \quad (14)$$

By substituting from Equation (13) into Equation (14) which yields:

$$S_T^n = \left(\frac{T^2}{n^2}\right)\bullet\left[A_2+\frac{\left(\lambda^2-A_{56}^2\right)A_4+2A_6A_{56}A_{34}}{\left(\lambda^2-A_{56}^2\right)^2}+\frac{A_8}{\left(\lambda^2-A_9^2\right)}\right] \quad (15)$$

Polymethyl-metha acrylate (PMMA) polymer material

The Sellmeier equation of the refractive-index is the form of:

$$n^2 = 1+\frac{C_1\lambda^2}{\lambda^2-C_2^2}+\frac{C_3\lambda^2}{\lambda^2-C_4^2}+\frac{C_5\lambda^2}{\lambda^2-C_6^2} \quad (16)$$

Where λ is in μm, the Sellmeier equation coefficients of Equation (16) are as the values (Ishigure et al., 1996):

C_1 = 0.4963, C_2 = 71.80 x 10^{-3}, C_3 = 0.6965, C_4 = 117.4 x 10^{-3}, C_5 = 0.3223 and C_6 = 9237 x10^{-3}.

Then the differentiation of Equation (16) w. r. t Wavelength (λ) gives:

$$\frac{\partial n}{\partial \lambda} = -(\lambda/n)\left[\frac{C_1C_2^2}{(\lambda^2-C_2^2)^2}+\frac{C_3C_4^2}{(\lambda^2-C_4^2)^2}+\frac{C_5C_6^2}{(\lambda^2-C_6^2)^2}\right] \quad (17)$$

In fact, the Spectral Sensitivity is defined as the following:

$$S_\lambda^n = \frac{\lambda}{n}\left(\frac{\partial n}{\partial \lambda}\right) \quad (18)$$

By substituting from Equation (17) into Equation (18) which yields:

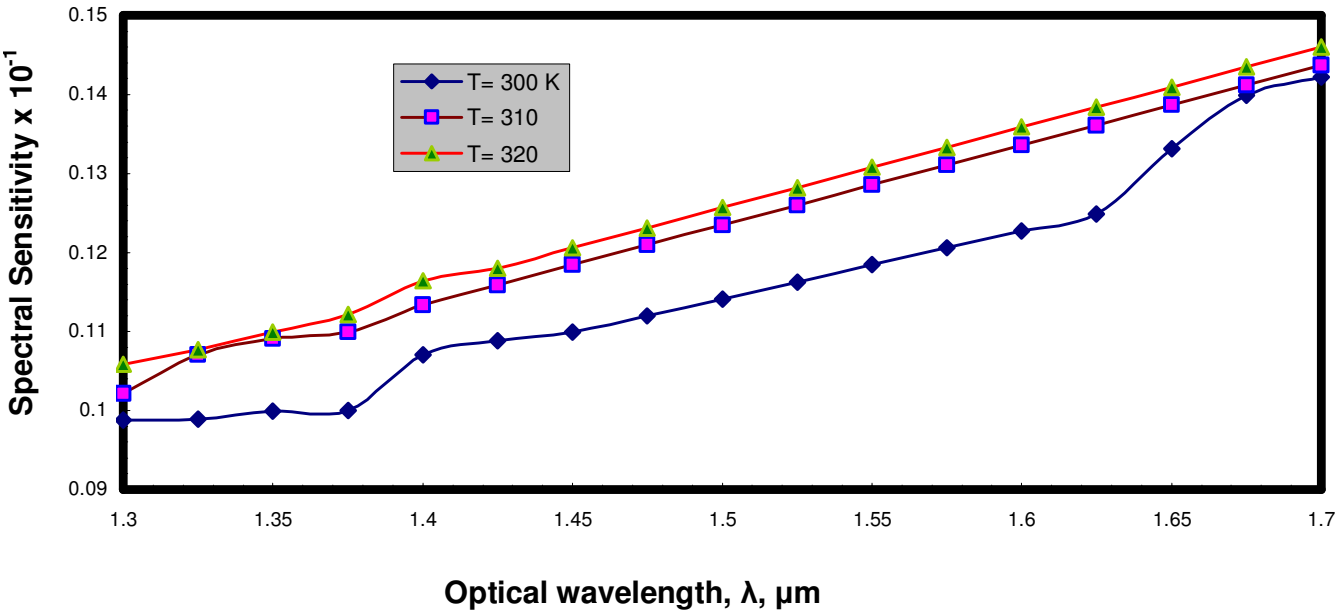

Figure 1. Variation of spectral sensitivity versus wavelength for Silica-doped material.

$$S_{\lambda}^{n} = -\left(\frac{\lambda^2}{n^2}\right)\left[\frac{C_1C_2^2}{(\lambda^2-C_2^2)^2}+\frac{C_3C_4^2}{(\lambda^2-C_4^2)^2}+\frac{C_5C_6^2}{(\lambda^2-C_6^2)^2}\right] \quad (19)$$

Also, the differentiation of Equation (16) w. r. t. Temperature (T) gives:

$$\frac{\partial n}{\partial T}=\left(-\lambda^2/n\right)\left[\frac{C_1C_2\frac{\partial C_2}{\partial T}}{(\lambda^2-C_2^2)^2}+\frac{C_3C_4\frac{\partial C_4}{\partial T}}{(\lambda^2-C_4^2)^2}+\frac{C_5C_6\frac{\partial C_6}{\partial T}}{(\lambda^2-C_6^2)^2}\right] \quad (20)$$

In fact, the Thermal Sensitivity is defined as the following:

$$S_T^n=\frac{T}{n}\left(\frac{\partial n}{\partial T}\right) \quad (21)$$

By substituting from Equation (20) into Equation (21) which yields:

$$S_T^n=\left(-\frac{T\lambda^2}{n^2}\right)\left[\frac{C_1C_2\frac{\partial C_2}{\partial T}}{(\lambda^2-C_2^2)^2}+\frac{C_3C_4\frac{\partial C_4}{\partial T}}{(\lambda^2-C_4^2)^2}+\frac{C_5C_6\frac{\partial C_6}{\partial T}}{(\lambda^2-C_6^2)^2}\right] \quad (22)$$

RESULTS AND DISCUSSION

Spectral Sensitivities variations of refractive-index (n) for three waveguides are displayed in Figures (1 - 6); these figures assure the following results:

1) As shown in Figures (1, 2), as the wavelength of Silica-doped material increases, the spectral sensitivity (multiplication in the order of 10^{-1}) of Silica-doped also increases at the constant temperature, and as the ambient Temperature increases, also the spectral sensitivity of Silica-doped increases at the constant Wavelength.
2) As shown in Figures (3, 4), as the wavelength of Lithium Niobate ($LiNbO_3$) material increases, the spectral sensitivity (multiplication in the order of 10^{-1}) of $LiNbO_3$ decreases at the constant temperature, and as the ambient Temperature increases, also the spectral sensitivity of $LiNbO_3$ increases at the constant Wavelength.
3) As shown in Figures (5, 6), as the wavelength of PMMA Polymer material increases, the spectral sensitivity(multiplication in the order of 10^{-1}) of PMMA Polymer material also increases at the constant temperature, and as the ambient Temperature increases, also the spectral sensitivity of PMMA Polymer material increases at the constant Wavelength.

Thermal Sensitivities variations of refractive-index (n) for three waveguides are displayed in Figures (7 - 12), these figures assure the following results:
4) As shown in Figures (7, 8), as the wavelength of Silica-doped material increases, the Thermal sensitivity (multiplication in the order of 10^{-4}) of Silica-doped also increases at the constant temperature, and as the ambient Temperature increases, also the Thermal

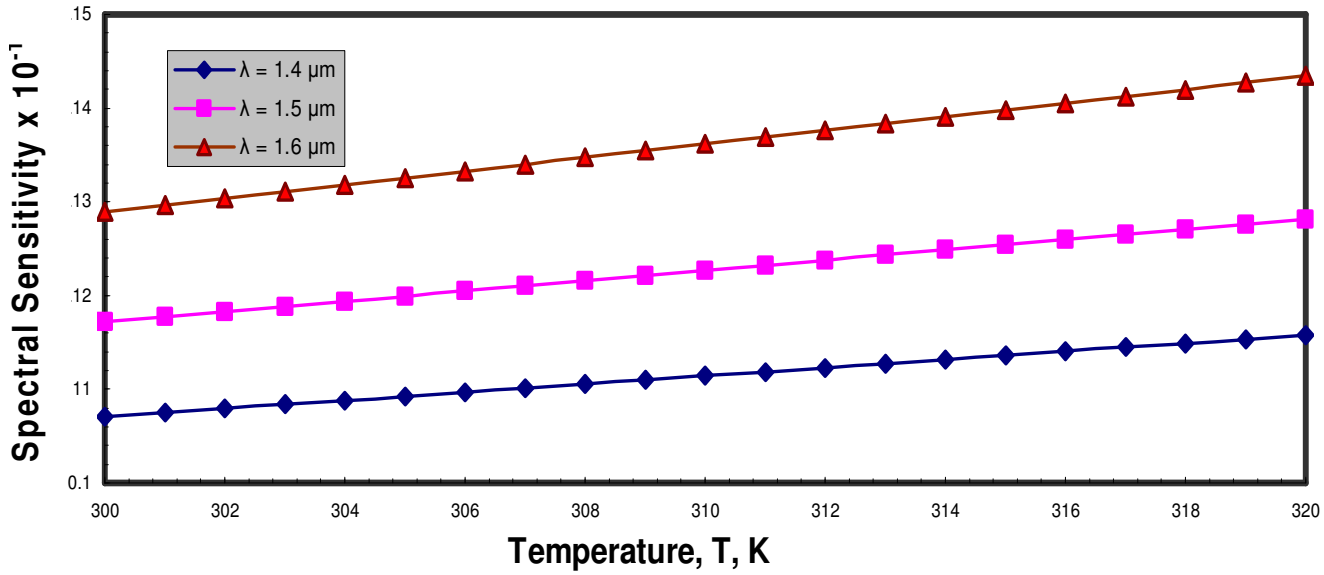

Figure 2. Variation of spectral sensitivity versus temperature for silica-doped material.

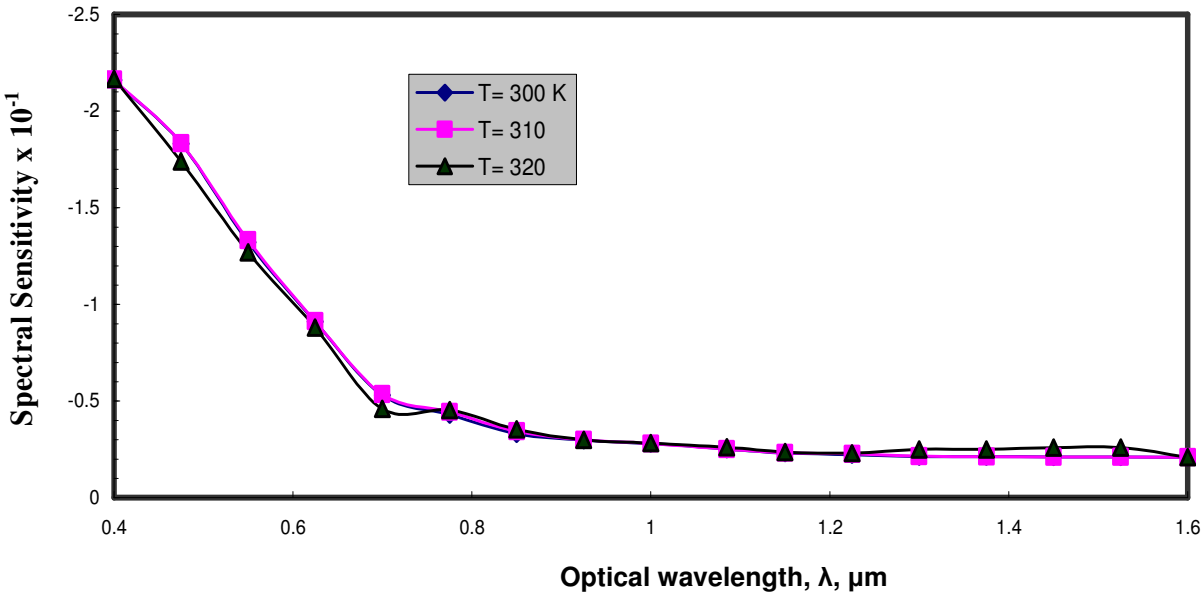

Figure 3. Variation of spectral sensitivity versus wavelength for $LiNbO_3$ material.

sensitivity of Silica-doped increases at the constant Wavelength.

5) As shown in Figures (9, 10), as the wavelength of Lithium Niobate ($LiNbO_3$) material increases, the Thermal sensitivity (multiplication in the order of 10^{-2}) of $LiNbO_3$ decreases at the constant temperature, and as the ambient Temperature increases, also the Thermal sensitivity of $LiNbO_3$ increases at the constant Wavelength.

6) As shown in Figures (11, 12), as the wavelength of PMMA Polymer material increases, the Thermal sensitivity (multiplication in the order of 10^{-4}) of PMMA Polymer material also decreases at the constant temperature, and as the ambient Temperature increases, also the Thermal sensitivity of PMMA Polymer material increases at the constant wavelength.

Conclusion

Silica-doped is the inorganic materials which have the highest spectral sensitivity, and medium thermal sensitivity than the other inorganic materials such as Lithium

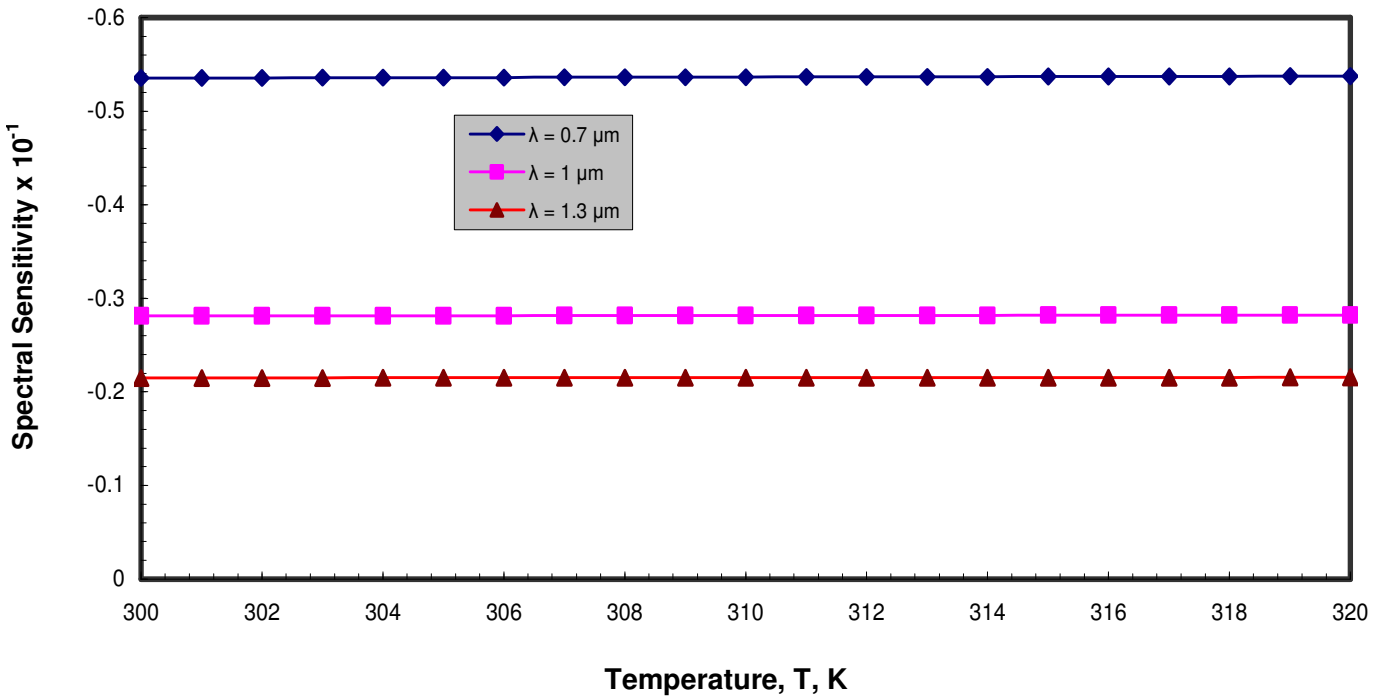

Figure 4. Variation of spectral sensitivity versus temperature for $LiNbO_3$ material.

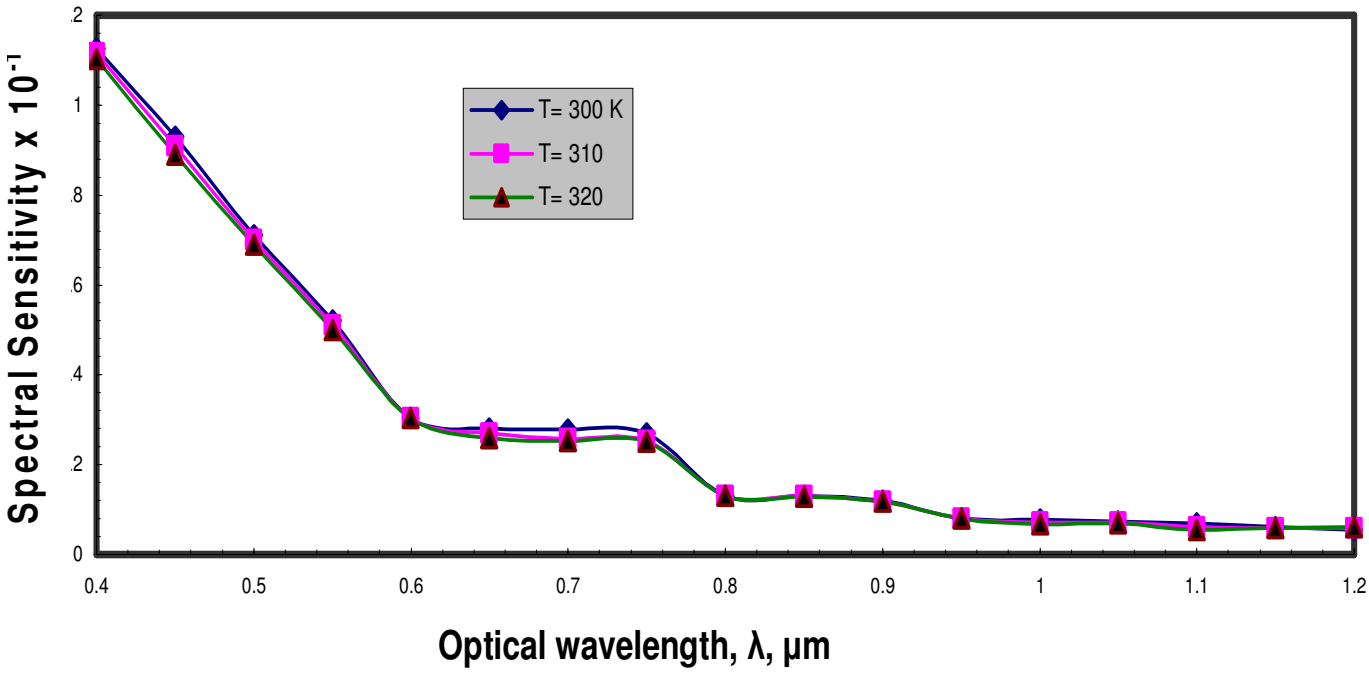

Figure 5. Variation of spectral sensitivity versus wavelength for PMMA material.

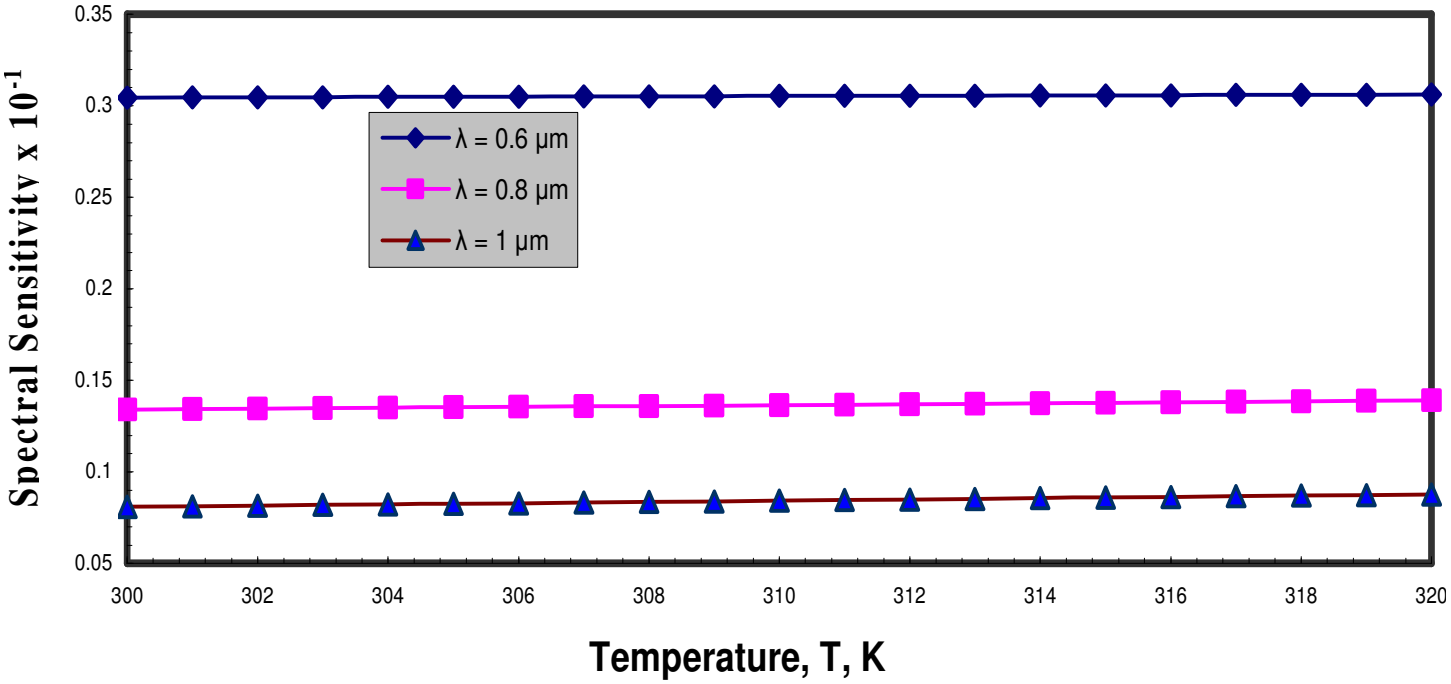

Figure 6. Variation of spectral sensitivity versus temperature for PMMA material.

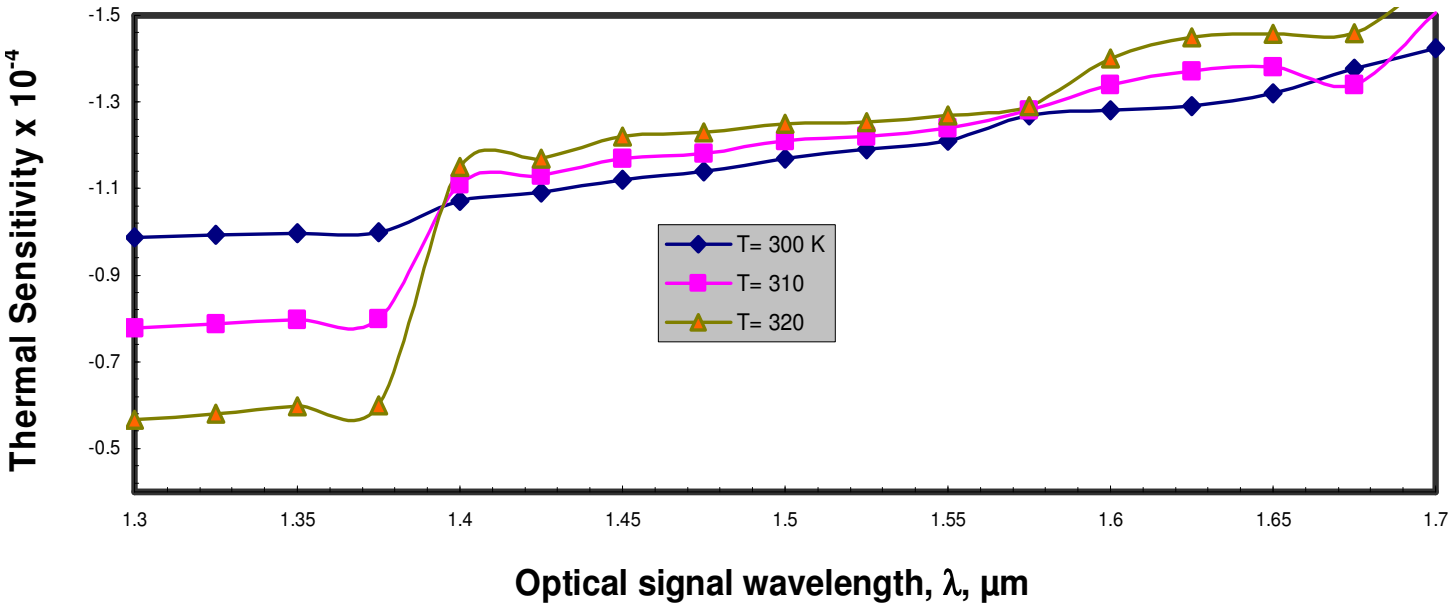

Figure 7. Variation of thermal sensitivity versus wavelength for silica-doped material.

Niobate ($LiNbO_3$) and organic materials such as PMMA Polymer under the conditions of the optical wavelength region and ambient temperature variations. From our study, we have concluded that silica-doped has the low propagation loss of the light, high reliability, and high spectral sensitivity, therefore silica-doped is the preferred based fabrication materials for conventional Arrayed Waveguide Grating (AWG) in Passive Optical Networks

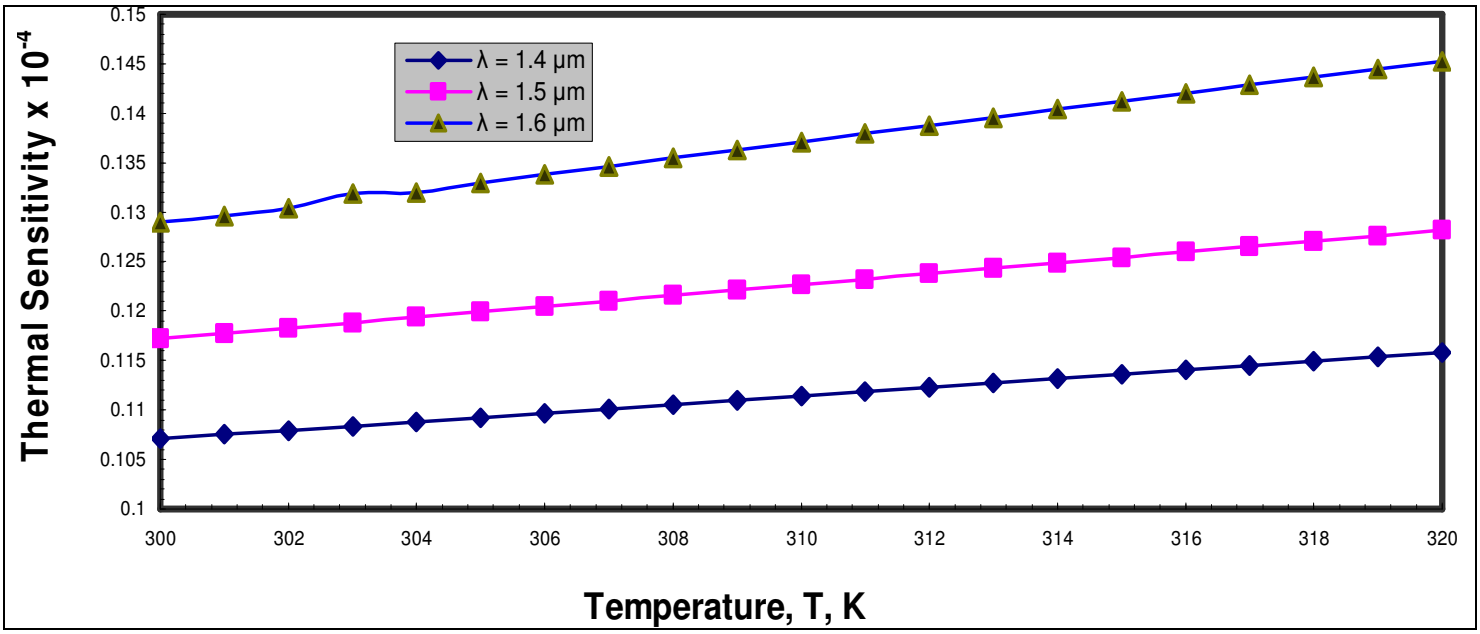

Figure 8. Variation of thermal sensitivity versus temperature for silica-doped material.

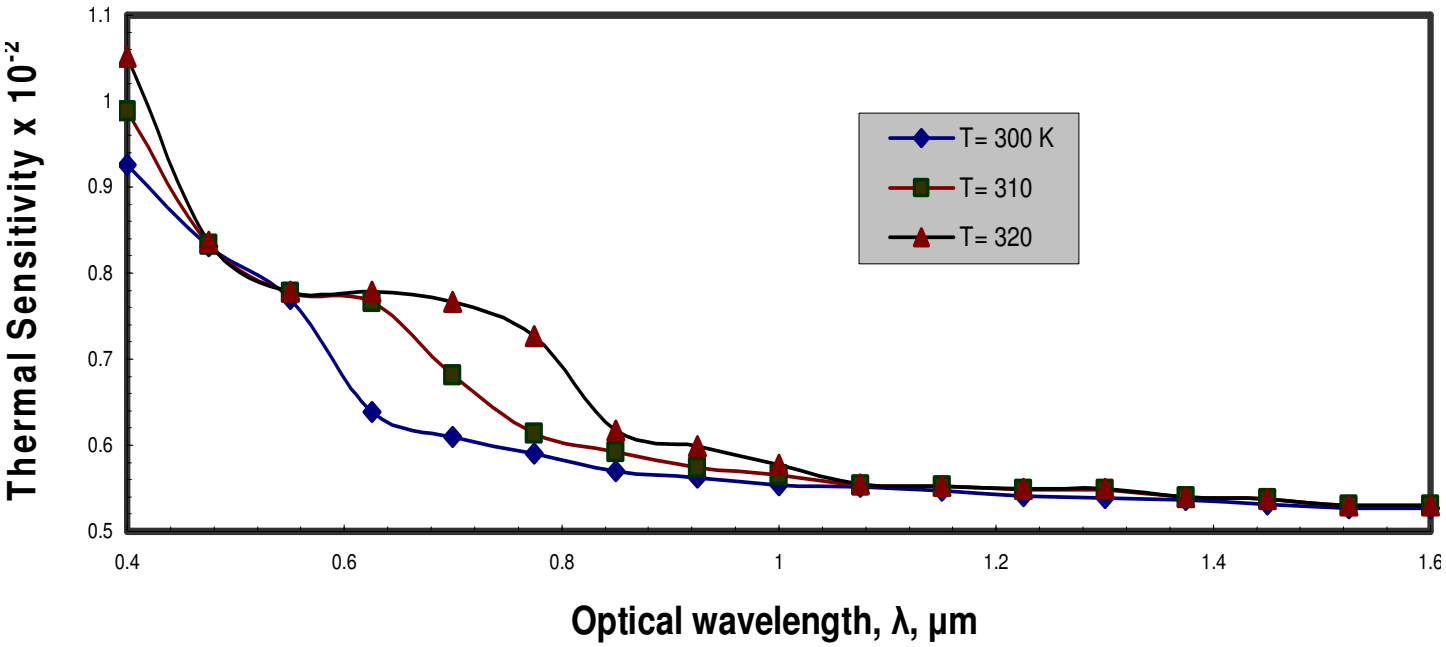

Figure 9. Variation of thermal sensitivity versus wavelength for $LiNbO_3$ material.

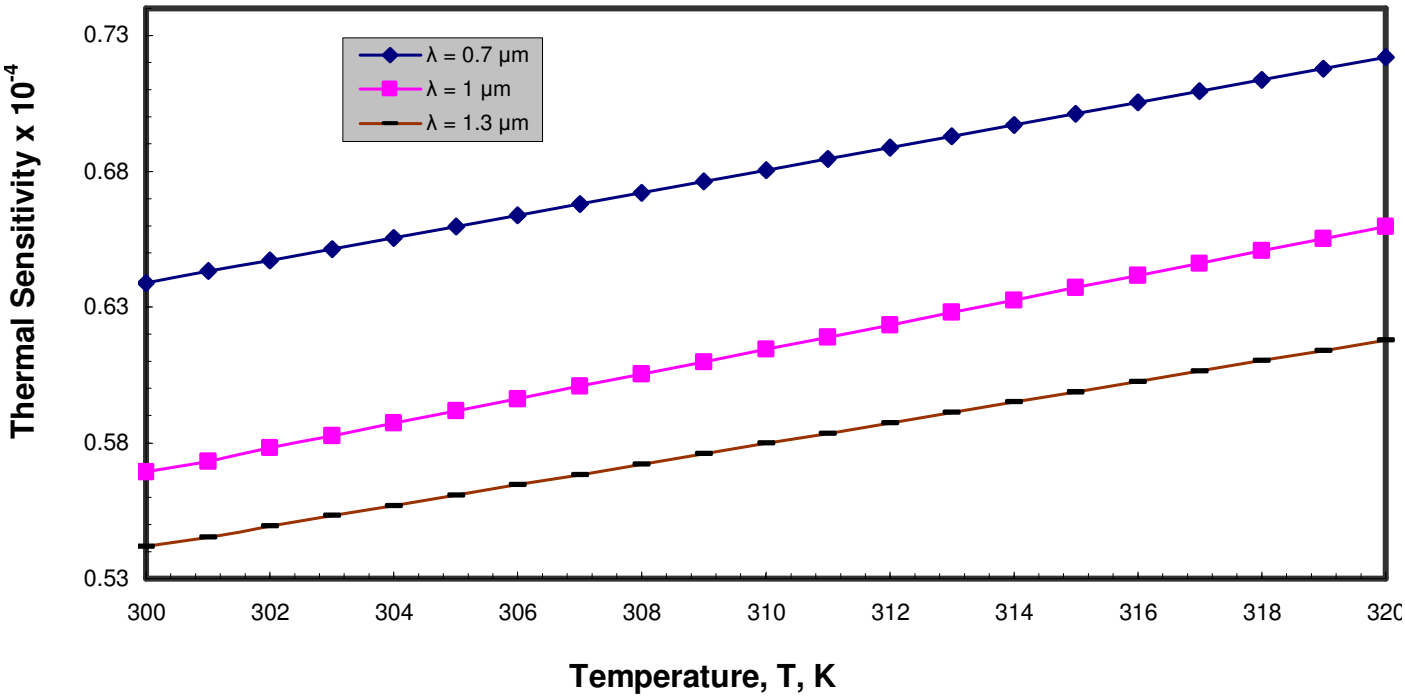

Figure 10. Variation of thermal sensitivity versus temperature for $LiNbO_3$ material.

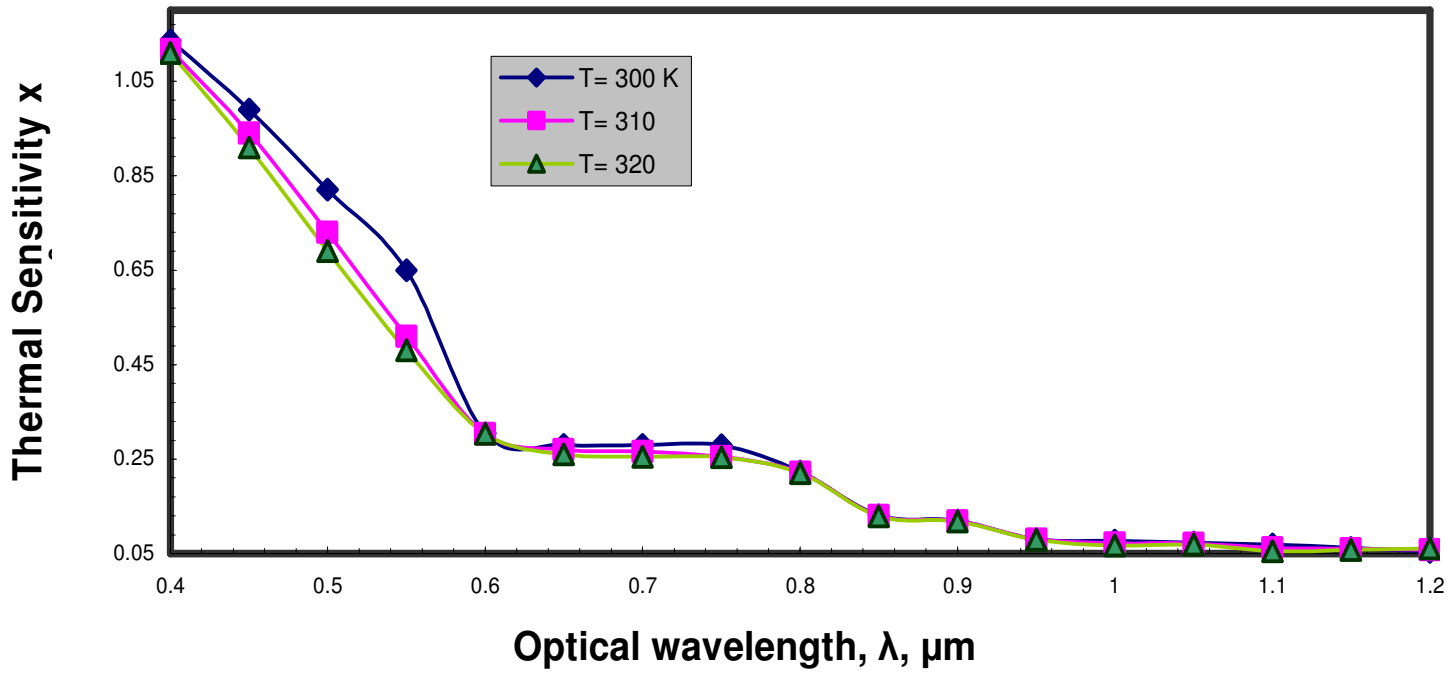

Figure 11. Variation of thermal sensitivity versus wavelength for PMMA material.

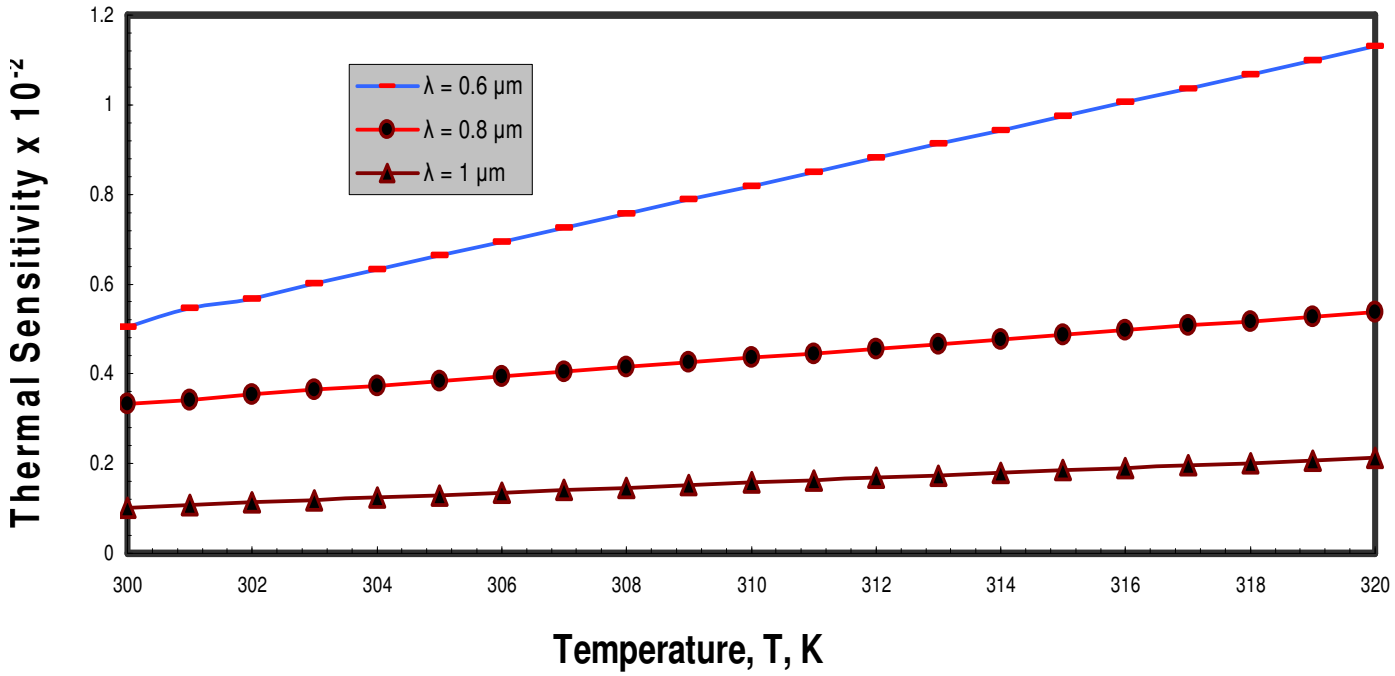

Figure 12. Variation of thermal sensitivity versus temperature for PMMA material.

(PONs) applications.

REFERENCES

Birks TA, Knight JC, Russell PSJ (1997). Endlessly Single-Mode Photonic Crystal Fiber, Opt. Lett. 15(22): 961–963.

MA CS, WANG XY (2004). An Efficient Technique for Analyzing Transmission Characteristics of Arrayed Waveguide Grating Multiplexers, Optical and Quantum Electronics 36(8): 759–71.

Humbert G, Malki A, Fevrier S, Roy P, Pagnoux D (2003). Electric-Induced Long-Period Gratings in Ge-free Air Silica Microstructure Fibers, Electron. Lett. 9(4): 349–350.

Ishigure T, Nihei E, Koike Y (1996). "Optimum Refractive Index Profile of the Grade-Index Polymer Optical Fiber, Toward Gigabit Data Link," Appl. Opt. 35(12): 2048-2053.

Jundt DH (1997). "Fabrication Techniques of Lithium Niobate Waveguides," Optics Letters, 22(9): 1553-1555.

Kakarantzas G, Birks TA, Russell PSJ (2002). Structural Long-Period Gratings in Photonic Crystal Fibers, Opt. Lett. 15(27): 1013–1015.

Kohtoku M, Takahashi H, Kitoh T, Shibata T, Inoue Y, Hibino Y (2002). Low-Loss Flat-Top Pass band Arrayed Waveguide Gratings Realized by First Order Mode Assistance Method, Electron. Lett. 38(15): 792–794.

Lee B (2003). Review of Present Status of Optical Fiber Sensors, Opt. Fiber Technol. 16(9): 57–79.

Maier M, Reisslein M (2004). AWG-Based Metro WDM Networking, IEEE Commun. Mag., 42(11): 19–26.

Smit MK, Van Dam C (1996). PHASAR-Based WDM-Devices: Principles, Design and Applications, IEEE J. Sel. Topics Quantum Electron. 2(2): 236–250.

Tsuda H, Okamoto, Ishii T, Naganuma K, Inoue Y, Takenouchi H, Kurokawa T (1999). Second- and Third-Order Dispersion Compensator Using a high-Resolution Arrayed-Waveguide Grating, IEEE Photon. Technol. Lett. 11(5): 569–571.

Uetsuka H (2004). AWG Technologies for Dense WDM Applications, IEEE J. Sel. Topics Quantum Electron. 10(2): 393–402.

van Eijkelenborg MA, Large MCJ, Argyros A, Zagari J, Manos S, Issa N, Bassett I, Fleming S, McPhedran RC, de Sterke CM, Nicorovici NAP (2001). Micro structured Polymer Optical Fiber, Opt. Exp. 13(9): 319–327.

Fleming W (1985). Dispersion in GeO_2-SiO_2 Glasses," Appl. Optics 23(24): 4486-4493.